Structural and Spectroscopic Studies of the Photophysical Properties of Benzophenone Derivatives

Brandi M. Baughman, Elana Stennett, Rachel E. Lipner, Andrew C. Rudawsky, and Sarah J. Schmidtke*

Department of Chemistry, College of Wooster, 943 College Mall, Wooster, Ohio 44691

Received: November 21, 2008; Revised Manuscript Received: May 8, 2009

The effect a solvent has on the photophysical properties of a series of benzophenone derivatives, all FDA approved for use in sunscreens, is examined. Experimentally significant differences in the solvatochromic behavior are found to be dependent upon the substituents on the parent benzophenone molecule. The spectral trends do not appear to originate from only changes in the solvent polarity but indicate that specific solvent−solute interactions influence the absorbance energies of some benzophenones. Computational investigations examine the structure and electronic excitation energies of the molecules. Specific interactions of the solvent and solute are modeled to evaluate structural changes that result from solvent−solute complexation and the impact of the changes upon absorbance properties. The viability of an intramolecular excited state proton transfer is theoretically evaluated. The combination of experimental and computational analysis provides a more complete understanding of the molecular level origin of the unique photophysical properties of this class of UV absorbers.

1. Introduction

There are many complexities in the origin and nature of spectroscopic transitions of condensed phase systems. Solvent−solute interactions, such as hydrogen bonding, influence the structure and reactivity of chemical systems such as proteins and host−guest complexes.[1−6] Hydrogen bonding interactions may preclude an intra- or intermolecular excited state proton transfer (ESPT), an efficient mechanism for decay following photoexcitation. Proton transfer reactions are a fundamental and widely investigated class of chemical reactions.[7−13] Previous experimental and theoretical studies have indicated the thermodynamics and kinetics of the ESPT have a dependence upon the solvent environment.[7−13] The systematic investigation of photophysical properties of molecules in the condensed phase and their molecular structure provides insight into the impact of interactions between the solvent and solute.

This investigation focuses upon benzophenone derivatives, an important class of organic molecules with applications as UV absorbers in personal care products. The three benzophenone derivatives examined (Figure 1) are all approved by the FDA for use in sunscreens: oxybenzone (OB), dioxybenzone (DOB), and sulisobenzone (SB).[14,15] OB is the most widely used in commercial personal care products, found in over half of sunscreens with SPF of 15 or higher.[14] The benzophenones are desirable sunscreen active ingredients due to their high molar absorptivity and ability to absorb radiation in both the UVA and UVB regions of the spectra.[15−17] On a molecular level the proximity of the carbonyl and hydroxyl groups in all three compounds allows for the formation of intra- and intermolecular hydrogen bonds. The ESPT mechanism is believed to provide an efficient excitation/deactivation cycle for the molecule, a useful property for sunscreens.[17] A fundamental understanding of the origin of the spectral behavior of organic UV absorbers is beneficial for the formulation of personal care products[16,17] and has applications in the detection and fate of the chemicals in the environment.[18,19]

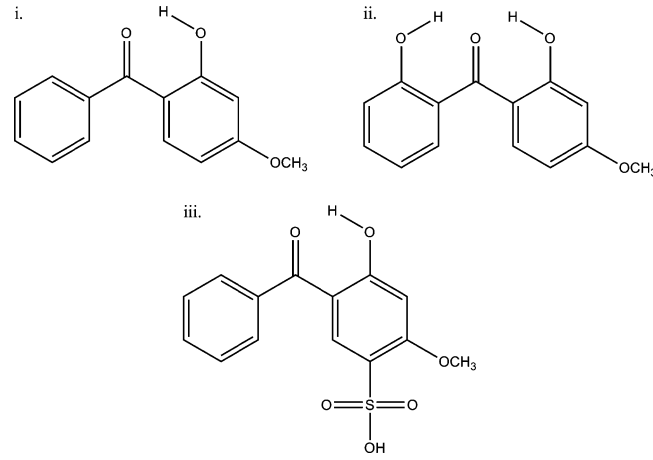

Figure 1. Structures of oxybenzone (i), dioxybenzone (ii), and sulisobenzone (iii).

Previous fundamental investigations, using semiempirical calculations to support spectroscopic data, reason that OB forms intramolecular hydrogen bonds in aprotic solvents, whereas intermolecular hydrogen bonds form between the solvent and the chromophore in protic solvents.[20−22] More recent investigations of sunscreen active ingredients, including OB, examined the Raman spectra as a function of solvent environment. Small shifts in the vibrational spectra with changes in the solvent polarity and hydrogen bonding ability were observed indicating weak interactions between OB and the solvent.[23] Related investigations of *o*- and *p*-hydroxy substituted benzophenones have considered the solvatochromism of the two lowest energy electronic transitions of the molecules.[24] The researchers classify the lowest energy absorbance as corresponding to a charge transfer from the hydroxyl oxygen to the carbonyl and the higher energy absorbance to a π to π^* transition localized on the phenyl

* Corresponding author: sschmidtke@wooster.edu; phone, (330)263-2359; fax, (330)263-2386.

10.1021/jp810256x CCC: $40.75
Published on Web 06/23/2009

moieties. The n to π^* transition was not observed in the hydroxyl-substituted benzophenones. It was found that the *o*-hydroxy derivative, similar to the series of benzophenones under investigation, had minimal solvatochromic shifts aside from in DMSO. Different solvatochromic shifts, resulting from changes in the solvent polarity, were observed in hydroxylic versus non-hydroxylic solvents for the π to π^* transition.[24]

In the past decade, studies of OB, DOB, and SB have been largely application driven, focusing upon the absorbance properties in oil- or alcohol-based matrixes like those used in personal care products.[16,17,25,26] In these studies, molecular properties are assumed from bulk properties rather than a comprehensive examination of the benzophenones on a molecular level, as can be done using quantum mechanical models. The present investigation utilizes modern quantum calculations to gain further insight into the molecular-level origin of the unique photophysical properties of this set of benzophenone derivates, with a focus on the role that solvent plays in the electronic transitions of the molecules.

The nature of solvent−solute interactions can be inferred from a chromophore's solvatochromism or spectral shifts accompanying changes in the solvent environment. It is important in solvatochromic studies to examine a wide range of solvents varying in properties such as solvent polarity and hydrogen-bonding ability, where the solvent acts as the proton donor and acceptor.[5,27] The treatment of the solvent as a bulk medium fails to account for specific interactions of the solvent with the solute or significant shifts in the charge distribution following photoexcitation.[23,28,29] To gain an accurate picture of the spectral events, it is necessary to consider specific interactions such as hydrogen bonding, solvent−solute complexation, changes in the electronic charge distribution following photoexcitation, and excited-state reactions. Using a combination of experimental and computational methods provides a more complete picture of the effects of solvent−solute interactions on the photophysical properties of the solute.[13,30,31]

We present a combination of spectroscopic and quantum mechanical calculations on the benzophenone derivatives. Experimentally the absorbance of the three molecules is measured in a wide range of solvents. Solvents are classified based upon their ability to form hydrogen bonds by hydrogen or electron pair donation, and solvents covering a range of polarities are used. The three molecules have unique responses to the different solvent environments. The results indicate that polarity alone is not able to account for the solvatochromic trends and that specific solvent−solute interactions play a role in the energy of electronic transitions. Quantum calculations are performed to examine the experimental results in greater detail. Excitation energies have been calculated using semiempirical, ZINDO, and time-dependent density functional theory, TD-DFT, methods.[32] Benzophenone:solvent complexes of DOB, OB, and SB with a single solvent molecule are investigated in terms of the complexation energies, structural changes due to complexation, and the electronic excitations of the complexed species relative to those of the free chromophore. The energetics of the proposed intramolecular ESPT is evaluated for all species.

2. Experimental Methods

2.1. Sample Preparation. Oxybenzone (Alfa Aesar, 99% pure), dioxybenzone (Aldrich, 98% pure), and sulisobenzone (Fluka, >97% pure) were used as received. Solutions (1.0×10^{-3} M) were made in ten solvents: acetonitrile (Pharmco-AAper, 99.9% pure), methanol (Pharmco-AAper, 100% pure), ethanol (AAper, 100% pure), 1-propanol (Sigma-Aldrich, 99.9% pure), 1-butanol (Sigma-Aldrich, 99.9% pure), dichloromethane (BDH, 99.5% pure), tetrahydrofuran (Pharmco, 99.7% pure), chloroform (BDH, 99.8% pure), carbon tetrachloride (EM, reagent grade), and toluene (Aldrich, 99% pure). For pH effects the following aqueous buffer solutions (1×10^{-2} M) were used: carbonate (pH 10), phosphate (pH 7), and acetate buffer (pH 4). Stock solutions were diluted to ensure the maximum absorbance, in the UV region, was between 0.2 and 1.0. Sulisobenzone solutions were not made in chlorinated solvents due to solute instability.

2.2. Spectral Measurements. Absorbance spectra were collected at room temperature on a Varian Cary 50 Bio Spectrophotometer. All spectra were corrected for solvent background by calibrating the instrument to the blank solvent or buffer solution. Spectra were taken in the range of 200−500 nm at a scan rate of 600 nm/min using the dual beam mode.

2.3. Computational Detail. Density functional optimizations and energy calculations were carried out using Gaussian03.[33] The geometries of each of the benzophenones, their proposed ESPT tautomers, and solvent complexes were optimized using density functional theory (DFT). The DFT method used was Becke's three parameter hybrid functional with the correlation functional of Perdew and Wang, B3PW91.[34,35] The Midi! basis set was used for all DFT optimizations.[36] Energies were determined through single point B3PW91/6-31+G(d,p) energy calculations. For the ESPT tautomers the OH bond distance was restrained to 0.97−1.02 Å to prevent back transfer during optimization of the ground tautomeric state. For the benzophenone/solvent complex energies basis set superposition error was determined using the counterpoise keyword.[32,33] The vibrational frequencies of the molecules were calculated to verify the nature of the stationary point. Excitation energies were calculated from the optimized ground states using time-dependent density functional theory (TD-DFT) methods, TD-B3PW91/6-31+G (d,p), to determine the first excited singlet state with nonzero oscillatory strength.[37,38] Gaussview 03 was used for visualization of computational work.[39]

The vertical excitation energies of the benzophenones were also calculated using ZINDO as implemented in ArgusLab 4.0.1.[40] The B3PW91/Midi! geometries were used as the starting point for the excitation calculations. Substitutions were allowed from the 10 highest HOMOs (highest occupied molecular orbitals) to the 10 lowest LUMOs (lowest occupied molecular orbitals). Solvation effects were evaluated using the SCRF Solvent Model,[40] an implicit solvent model based on the dielectric constant and refractive indices of each solvent, as well as the solvent cavity. If solvents were not found in the program default list, then the Minnesota Solvent Descriptors database was utilized.[41] The solvent cavity size was calculated by the program based upon the molecular size.

3. Results

3.1. Spectral Measurements. ***3.1.1. Solvent Effects.*** The absorbance spectra for OB are shown in Figure 2, those for DOB in Figure 3, and those for SB in Figure 4. The solvents used, including classification and solvent descriptors, are listed in Table 1. For comparison purposes the maximum absorbance is normalized to 1 for all measurements. Protic solvents (ROH) are shown with dashed lines, electron pair donating solvents (THF and CH_3CN) with dotted lines, and those with no specific solvent−solute interactions (toluene, CCl_4, $CHCl_3$, CH_2Cl_2) as solid lines.

For OB, all spectra show two absorbance maxima separated by about 4000 cm^{-1} in the UVA and UVB regions of the spectra,

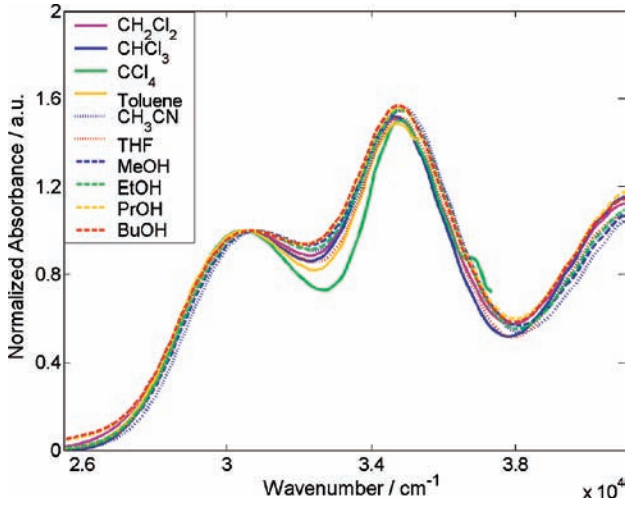

Figure 2. Normalized absorbance spectra for oxybenzone in a series of solvents.

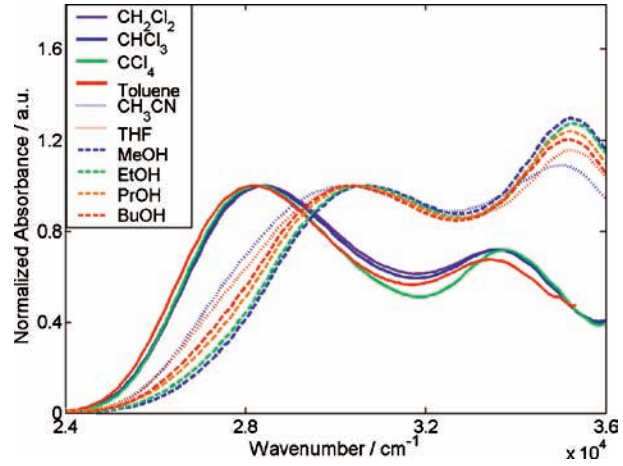

Figure 3. Normalized absorbance spectra for dioxybenzone in a series of solvents.

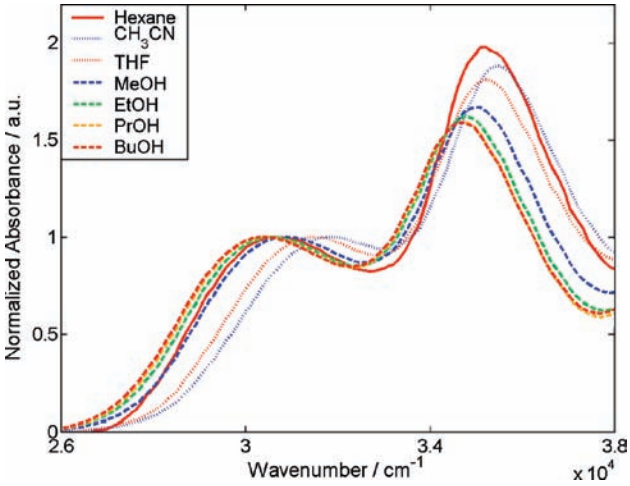

Figure 4. Normalized absorbance spectra for sulisobenzone in a series of solvents.

with the more intense absorbance at the higher energy. The absorbance bands of DOB exhibit solvent-dependent absorbance energies and variations in the intensity of the two bands relative to one another. In solvents without specific solvent−solute interactions, the absorbance bands are separated by about 5000 cm^{-1} with the lower energy band having greater intensity. Both absorbance bands have a blue shift of approximately 2000 cm^{-1} upon going to protic solvents. Electron pair donating solvents have absorbance bands at slightly lower energies than those of the protic solvents. In solvents with specific solvent−solute interactions, the higher energy transition is the more intense UV absorbance. SB shows two absorbance bands with a notable blue shift (1500 cm^{-1}) upon going to electron pair donating solvents. The absorbance bands are spaced by about 4100 cm^{-1} in the alcohols and the spacing decreases in electron pair donating solvents. In all solvents, the higher energy UV absorbance has the greatest intensity.

TABLE 1: Solvents Used in the Solvatochromic Studies

solvent[a]	ε[b]	E_T^N	α	β	class[c]
dichloromethane (CH_2Cl_2)	8.93	0.309	0	(0.30)	NSI
chloroform ($CHCl_3$)	4.7113	0.259	0	(0.44)	NSI
carbon tetrachloride (CCl_4)	2.2280	0.0502	0	0	NSI
toluene	2.3741	0.099	0.11	0	NSI
hexane	1.8819	0.009	0	0	NSI
acetonitrile (CH_3CN)	35.688	0.460	0.31	0.19	EPD
tetrahydrofuran (THF)	7.4257	0.207	0.55	0	EPD
methanol (MeOH)	32.613	0.762	(0.62)	0.93	protic
ethanol (EtOH)	24.852	0.654	(0.77)	0.83	protic
propanol (PrOH)	20.524	0.617		0.78	protic
butanol (BuOH)	17.332	0.586	(0.88)	0.79	protic

[a] Abbreviations used for each solvent are given following the solvent. [b] Dielectric constants (ε) from ref 41, normalized electronic transition energies (E_T^N) from ref 42, and acidity (α) and basicity (β) from ref 43. Values in parentheses are reported as less certain. [c] Classification of solvent type: NSI = no specific solvent−solute interactions, EPD = electron pair donating.

TABLE 2: Experimentally Measured Absorbance Maxima for Oxybenzone, Dioxybenzone, and Sulisobenzone

	oxybenzone		dioxybenzone		sulisobenzone	
solvent	$S_0 \rightarrow S_1$ cm^{-1}	$S_0 \rightarrow S_2$ cm^{-1}	$S_0 \rightarrow S_1$ cm^{-1}	$S_0 \rightarrow S_2$ cm^{-1}	$S_0 \rightarrow S_1$ cm^{-1}	$S_0 \rightarrow S_2$ cm^{-1}
CH_2Cl_2	30586	34727	28410	33565	[b]	
$CHCl_3$	30484	34595	28323	33565	[b]	
CCl_4	30491	34850	28323	33779	[b]	
toluene	30483	34727	28174	33442	[a]	
hexane	[a]		[a]		30583	35205
CH_3CN	30863	34837	30209	34975	31846	35458
THF	30586	34727	30303	35216	31450	35216
MeOH	30866	34841	30672	35207	30863	34971
EtOH	30762	34841	30584	35207	30578	34717
PrOH	30673	34727	30396	35207	30483	34727
BuOH	30586	34727	30303	35216	30397	34727

[a] Compound had limited solubility. [b] Solutions were unstable.

Table 2 summarizes the experimentally measured absorbance maxima for the low energy ($S_0 \rightarrow S_1$) and higher energy ($S_0 \rightarrow S_2$) transitions in all solvents for the benzophenones. For OB, the low energy transition blue shifts with increasing solvent polarity and no clear trend is observed for the high-energy transition. In DOB, a blue shift is observed with increasing solvent polarity within solvents that have similar solvent−solute interactions. There is a significant increase in the absorbance energy upon going from solvents that have no specific interactions to either protic or electron pair donating solvents. The higher energy transition shows a significant blue shift upon going to solvents with specific solvent−solute interactions but has a less noticeable trend in solvatochromism within a given class of solvents. SB has similar blue shifts with increasing solvent polarity as observed in OB and DOB, as well as a significant increase in the absorbance energy upon going to electron pair donating solvents (CH_3CN and THF).

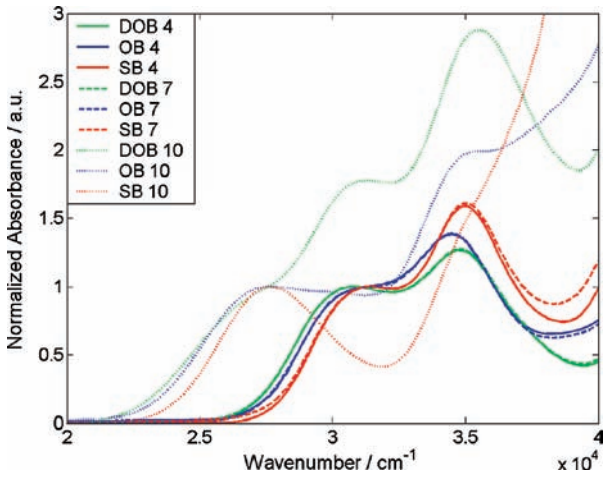

Figure 5. Normalized absorbance spectra for oxybenzone (OB, blue), dioxybenzone (DOB, green), and sulisobenzone (SB, red) in aqueous buffers. The acetate buffer (pH = 4) is shown as a solid line, phosphate buffer (pH = 7) as a dashed line, and carbonate buffer (pH = 10) as a dotted line.

3.1.2. pH Effects. The effect of solvent pH was analyzed for all species in aqueous buffer solutions. The spectra for OB, DOB, and SB in an acidic, basic, and neutral buffer are shown in Figure 5. Similar absorbance profiles are observed for all species under neutral and acidic conditions. There is a significant red shift in the absorbance energy (3000 cm^{-1}) and change in the absorbance profile upon changing to basic conditions.

3.2. Computational Analysis. ***3.2.1. Free and Complexed Benzophenone Geometries.*** B3PW91/Midi! geometry optimizations were performed in the gas phase for OB, DOB, and SB. Comparison of the gas and solution phase DOB:MeOH optimized complexes, reported in the Supporting Information, indicate negligible structural changes with the inclusion of bulk solvent model; therefore gas phase calculations are believed to provide an accurate complex analysis. Results are summarized in Table 3, and Figure 6 shows the optimized structures with labels for angles and bonds of interest. Explicit solvent−solute complexes were considered for three solvents: methanol (MeOH), acetonitrile (CH_3CN), and tetrahydrofuran (THF). Representative B3PW91/Midi! optimized 1:1 solvent−solute complexes are found in the Supporting Information, with important bond lengths and angles summarized in Table 3. For complexes, the MeOH was positioned to form a hydrogen bond to the central carbonyl of the benzophenone, and electron-pair-donating solvents (THF, CH_3CN) positioned with the free electron pair on the solvent pointed toward the hydroxyl proton of the benzophenone. The hydrogen bond lengths (β) and angles (θ_{HB}) indicate formation of the strongest hydrogen bonds with MeOH, followed by those of THF, and weakest bonding with CH_3CN.[1] In OB and SB, minimal structural changes were observed upon complexation. In DOB, a significant increase in the dihedral angle (Θ) between the two ring moieties with complexation, and the largest change in the torsion angle occurs in the DOB:MeOH complex relative to that of free DOB.

The strength of the complexes was considered by comparing the B3PW91/6-31+G(d,p)//B3PW91/Midi! energy of the solvent/solute complex with the sum of the free solvent and free benzophenone. Table 3 summarizes the gas phase complexation energies, including basis set superposition errors (BSSE), where a negative value indicates an energetically favorable complexation.

A final consideration for SB is the role of the sulfonic acid group. On the basis of the acidity of this group in unbuffered solvents, the SB exists in the deprotonated form, as is supported by the low pH of aqueous solutions of SB. Optimizations were carried out for the deprotonated sulfonic acid group. Minimal structural changes were observed for the anionic species relative to neutral SB.

3.2.2. Excited State Properties. The excitation energies of the free and complexed benzophenones were evaluated using ab initio and semiempirical methods, for comparison with spectral measurements. The dipole moments of the ground and excited states involved in the observed transitions were evaluated to provide insight into observed solvatochromic shifts. Table 4 summarizes the calculated gas phase TD-B3PW91/6-31+G(d,p) excitation energies, ZINDO excitation energies, and dipole moments for the electronic states from the ZINDO calculations. Inclusion of different solvent environments, modeled based upon the solvent dielectric and index of refraction, resulted in minimal solvatochromic shifts. Comparison of the vertical excitation energy in the gas phase versus in a polar solvent (CH_3CN) shows the dipole moments of the ground and first single excited states exhibit small changes upon excitation. For this reason bulk solvent−solute interactions are similar for both electronic states resulting in minimal calculated solvatochromic shifts. A comparison of oscillatory strengths for the first two electronic transitions, relative to absorbance cross sections, for the different solvent classes are reported and assessed in the Supporting Information.

Comparison of excitation energies of the free and benzophenone:solvent complexes yields larger shifts in the excitation energies. In OB minimal absorbance energy changes are observed for the free versus complexed species. For DOB a blue shift of ca. 1600 cm^{-1} is observed upon going to the DOB:MeOH complex from the free DOB based upon ZINDO calculations, with a lesser magnitude increase calculated by TD-DFT. SB has energetic shifts between these two extremes upon complexation. Complexation with electron pair donating solvents, based upon ZINDO calculations, results in no change with MeOH and an increase in the excitation energy for SB complexes with both electron pair donating solvents.

For SB the absorbance energies were evaluated for the fully deprotonated species, as well as a neutral species that is deprotonated at the sulfonic acid and has an acidic proton in the proximity of the benzophenone carbonyl group (Table 4). ZINDO calculations predict that deprotonation of the SB results in decreased absorbance energy relative to the neutral species. Both TD-DFT and ZINDO calculations predict that association of the proton with the SB, near the carbonyl group, lowers the excitation energy of SB relative to the anion.

3.2.3. Intramolecular Excited State Proton Transfer. In the gas phase, the thermodynamics of the ESPT process, illustrated in Figure 7, were analyzed using DFT and TD-DFT calculations. Table 5 summarizes the relative energies of the ground and first excited states of the normal and ESPT tautomers in their S_0 and S_1 electronic states. The ground state energies are the B3PW91/6-31+G(d,p)//B3PW91/Midi! energies, referenced to the energy of the normal species. The excited state energies are found by adding the TD-B3LYP/6-31+G(d,p) vertical excitation energy to that of the optimized ground state. For OB and SB there is only one site for an intramolecular ESPT, between the central carbonyl and adjacent hydroxyl group, and the process is thermodynamically favorable in the ES, but not the ground state. In DOB there are two possible intramolecular ESPT sites, depending upon the hydroxyl group from which the transfer occurs. For both sites the transfer is not thermodynamically favorable in the ground or excited state.

TABLE 3: Calculated Geometries and Complexation Energies (*E*) for Free and 1:1 Solute:Solvent Complexes

		free	MeOH	THF	CH_3CN
oxybenzone	α[a]	1.539	1.548	1.619	1.573
	β		1.840	2.318	2.864
	θ	153.7	153.2	146.8	150.5
	θ_{HB}		159.2	113.5	107.0
	Θ	45.0	43.5	44.7	43.5
	E		−9.123	−5.979	8.135
dioxybenzone[b]	α_1	1.574	1.558 (2.677)	1.515 (1.714)	1.544 (1.577)
	α_2	1.584	2.677 (1.558)	1.860 (1.562)	1.653 (1.574)
	β_1		1.676 (1.676)	1.987 (2.106)	2.571 (3.066)
	β_2		1.545 (1.545)		
	θ_1	151.6	152.8 (100.8)	153.7 (140.8)	152.3 (149.2)
	θ_2	151.0	100.8 (152.8)	134.8 (151.7)	145.8 (150.2)
	θ_{HB}		155.7 (155.7)	128.6 (120.7)	122.9 (132.2)
			172.2 (172.2)		
	Θ	37.4	53.1 (53.1)	41.0 (38.8)	37.4 (36.4)
	E		0.908 (6.132)	−0.337 (−4.728)	4.495 (5.486)
sulisobenzone[c]	α	1.502	1.516	1.525 (1.506)	1.555 (1.507)
	β		1.868	3.262 (1.570)	2.717 (1.957)
	θ	154.1	153.6	152.4 (154.3)	150.4 (154.2)
	θ_{HB}		158.8	107.7 (160.9)	110.8 (165.3)
	Θ	40.4	42.0	40.6 (40.8)	41.2 (40.2)
	E		−6.630	−11.487 (−38.116)	3.999 (−23.271)

[a] Figure 6 illustrates measurements and complexes of interest. Bond lengths are given in angstroms, angles in degrees, and energies in kJ/mol. All measurements from B3PW91/Midi! optimized geometries and energies are B3PW91/6-31+G(d,p)//B3PW91/Midi! including BSSE. [b] Where two values are given, the first value corresponds to a 1:1 complex bonding at the phenyl group without the methoxy and the value in parentheses corresponds to bonding to that with the methoxy. [c] Where two values are given, the first value corresponds to a 1:1 complex at the hydroxyl and the value in parentheses corresponds to bonding at the sulfonic acid group.

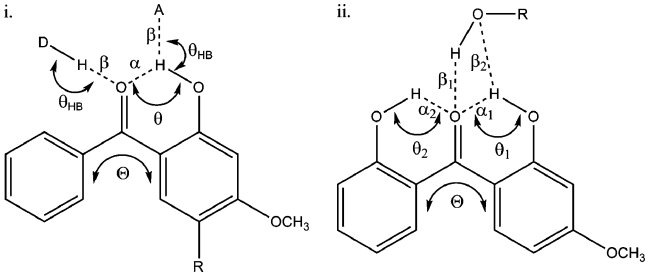

Figure 6. Bond lengths and angles of interest for the benzophenones. Oxybenzone and sulisobenzone correspond to (i). Dioxybenzone labels, which differ from (i), are shown in (ii). In (i) A = hydrogen bond acceptor in solvent complex, D = hydrogen bond donor in solvent complex, and R = H or SO_3H, and in (ii) R = CH_3.

4. Discussion

4.1. Solvatochromism. For each molecule we consider the origin of the experimentally observed solvatochromic shifts in light of a molecular level view of solvent−solute interactions. The calculations estimate structural changes upon solvent−solute complexation, the favorability of complexation, and the impact upon the electronic properties of the chromophore.

4.1.1. Oxybenzone. OB exhibits minimal solvatochromic shifts (Table 2, Figure 2). There is a small blue shift with increasing solvent polarity. The dipole moments of the ground (S_0) and excited state (S_1) of OB are nearly identical, with a slight decrease of less than ca. 0.02 D in the gas phase. Dielectric interactions between the solvent and solute would lead to similar energetic shifts of the relative energies of the two electronic states. One explanation of the solvatochromic trends is that the (slightly) less polar first electronic state is less stabilized than the ground state in polar solvents. For this reason a small blue shift, or increased energy gap between electronic states, is observed as solvent polarity increases. For OB the solvent dielectric constants[41] and Reichardt's solvatochromic scale[42] (Table 1) can be used to predict solvatochromic trends, indicating that bulk solvent−solute interactions result in the observed spectral shifts. In general there is a direct relationship between the solvent polarity and absorbance energy.

The excitation energy calculations indicate the first observed transition is predominantly HOMO to LUMO in character, and the second electronic transition HOMO-1 to LUMO. The molecular orbitals of interest are shown in Figure 8. Both transitions have an additional nodal surface in the ring moiety for the hydroxyl ring, indicative of π to π^* character. The HOMO to LUMO transition is accompanied by a change in the electron density on the hydroxyl and carbonyl oxygens, whereas this change is localized to only the ring moiety for the higher energy HOMO-1 to LUMO transition. Following a HOMO to LUMO electronic excitation, the proton is likely to transfer from the hydroxyl to the carbonyl group (ESPT), due to the changes in the electron density. These results are in agreement with the assignment of the low and high energy bands for the *o*-hydroxy-substituted benzophenone, previously reported, in which the low energy excitation is assigned to a charge transfer and the higher energy excitation the π to π^* transition of the ring moiety.[24]

Analysis of explicit solvent−solute complexation indicates that formation of hydrogen bonds is favorable for OB with both electron pair donating solvents and protic solvents. In both cases negligible structural changes accompany complexation; therefore the excitation energies of the solvent complexes are nearly the same as that of the uncomplexed species. So although it is likely that solvent-not/solute complexes are formed by OB in protic and electron pair donating solvents, it is not readily apparent from its absorbance properties. Previous investigations using Raman spectroscopy[23] and a linear correlation of the hydroxyl chemical shift with the absorbance maxima[20] indicate interactions, such as hydrogen bonding, between OB and protic solvents.

4.1.2. Dioxybenzone. DOB exhibits significant solvatochromic shifts related to the solvent's ability to form explicit solvent−solute bonds. A blue shift of approximately 2500 cm^{-1}

TABLE 4: Calculated Dipole Moments and Vertical Transition Energies for Free and 1:1 Solute:Solvent Complexes

		dipole moment[a]		vertical excitation energy[b]		
		S_0	S_1	TD-DFT (g)	ZINDO (g)	ZINDO (l)
oxybenzone	free	7.63	7.60	29447	31410	31688
	MeOH	8.18	9.48	29000	31198	31106
	THF	6.80	6.58	29688	31842	32081
	CH_3CN	4.42	3.94	29599	31617	31752
dioxybenzone [c]	free	7.77	8.72	27061	29701	29409
	MeOH	5.89	7.07	27835	31312	31108
		(6.06)	(7.57)	(27396)	(30838)	(30451)
	THF	7.48	8.31	27270	30731	30566
		(6.22)	(7.14)	(27548)	(30440)	(30245)
	CH_3CN	4.05	4.77	27149	30097	29977
		(5.16)	(5.51)	(27400)	(29899)	(29509)
sulisobenzone [d]	free	5.94	6.97	30721	32045	31890
	MeOH	6.52	8.14	30283	32051	31670
	THF	6.06	7.20	30712	32732	32617
		(5.89)	(7.97)	(30626)	(32125)	(31787)
	CH_3CN	9.98	10.38	30665	32498	32476
		(5.70)	(8.47)	(30673)	(32044)	(31549)
	anion			32229	30774	
	anion-H^+			27544	23462	

[a] Dipole moments from ZINDO calculation in the gas phase and reported in debye. [b] TD-DFT vertical excitation energies from TD-B3PW91/6-31+G(d,p) calculations in gas phase and ZINDO calculations in gas phase (g) or with acetonitrile solvation (l). Energies are reported in cm^{-1}. [c] Where two values are given, the first value corresponds to 1:1 complex bonding at the phenyl group without the methoxy and in parentheses that with the methoxy. [d] Where two values are given, the first value corresponds to 1:1 complex at the hydroxyl and in parentheses at the sulfonic acid group. For comparison the gas phase excitations energies, for the same MO transitions, are reported for the anion resulting from deprotonation at the sulfonic acid group (anion) and the anion with association of the free proton near the carbonyl (anion$-H^+$).

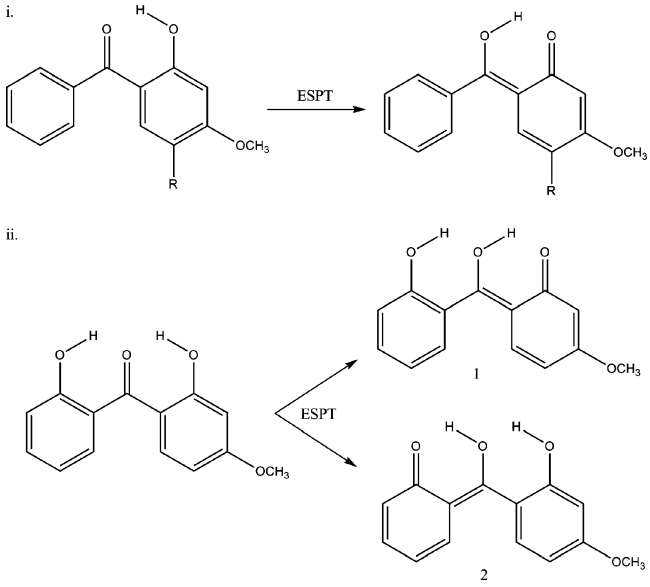

Figure 7. Schematic of the intramolecular excited state proton transfer. The reactant is referred to as the normal species and the product referred to as the tautomer. Oxybenzone (R = H) and sulisobenzone (R = SO_3H) are shown in (i) and dioxybenzone is shown in (ii).

is observed upon going to protic solvents and 2000 cm^{-1} upon going to electron-donating solvents from nonpolar solvents such as chloroform. The experimentally observed solvatochromic trends do not correlate with the predicted bathochromic shift based upon DOB's ground and excited state dipole moments. Calculations indicate that the ground state (S_0) is less polar than the first electronic excited state (S_1); therefore, on the basis of bulk electrostatic interactions, more polar solvents will stabilize the excited state to a greater extent than the ground state resulting in a smaller energetic gap between the electronic states in more polar solvents.

Deviations in the observed spectral shifts relative to trends predicted by consideration of solvent dielectric constants (ε)

TABLE 5: Calculated Energetics of an Intramolecular Excited State Proton Transfer Energetics

		S_0[a]	S_1
oxybenzone	normal	0	29157
	tautomer	3275	27543
dioxybenzone	normal	0	27060
	tautomer 1	4218	27907
	tautomer 2	4266	27810
sulisobenzone[b]	normal	0	30721
	tautomer	2452	28778

[a] Energies reported in cm^{-1} and referenced to the normal species ground state. Ground state B3PW91/6-31+G(d,p)//B3PW91/Midi! energies and excited state TD-B3PW91/6-31+G(d,p) vertical excitation energies. [b] Species as illustrated in Figure 8.

and normalized electronic transition energies (E_T^N), Table 1, can be explained in part through consideration of specific solvent−solute interaction, such as complexation, in solvents that can form hydrogen bonds with the chromophore. The hydrogen bonding ability is accounted for in the acidity (α) and basicity (β), Table 1, of the solvents.[43] It is seen that, aside from toluene, solvents with nonzero acidities are blue shifted relative to nonacidic solvents. The higher acidity of the alcohols corresponds to the greater shift for protic versus electron pair donating solvents.

On a molecular level in protic solvents, such as the alcohol series examined, the central carbonyl group of DOB can act as a hydrogen bond acceptor for the alcohol's hydroxyl proton. In order for the intermolecular hydrogen bond to form, the intramolecular hydrogen bond of DOB must be perturbed. Calculations indicate that this is not energetically favorable in the gas phase, but in solvent, where hydrogen bonding networks can form, this may be a favorable process. The assumption that this occurs is supported by the observed spectral shifts in the alcohol solutions. Theoretical evaluation of absorbance energies indicate an increase in the excitation energy of DOB:MeOH complex relative to that of free DOB, correlating with the experimentally observed trend. This is the result of the increased

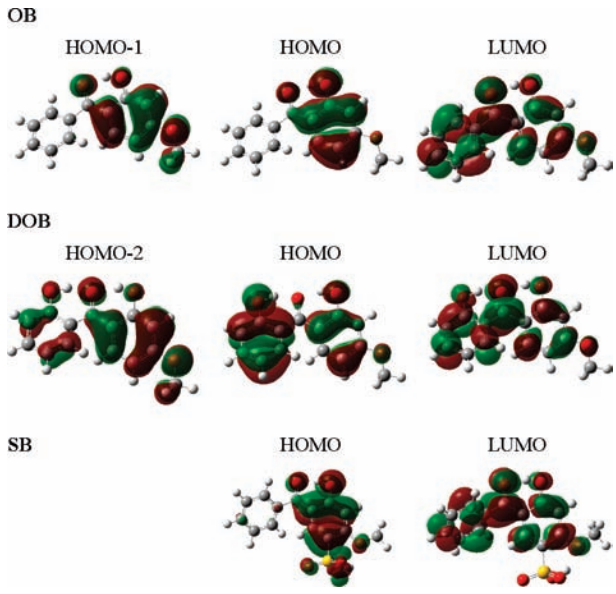

Figure 8. Molecular orbitals of interest for the spectral transitions of the benzophenones from the B3PW91/Midi! optimizations.

torsion angle, ca. 15.7°, of DOB in its complexed form. A smaller change in the torsion angle is observed upon complexation with electron pair donating solvents (CH_3CN and THF). In these cases the solvent electron pair acts as a proton acceptor for the hydroxyl proton(s) of DOB. This interaction reduces the strength of the intramolecular hydrogen bond but does not necessitate as significant of a structural change for the chromophore. In the ZINDO excitation energies a blue shift is observed upon complexation for both protic and electron pair donating solvents, with a greater shift for protic solvents as is experimentally determined.

The specific solvent−solute interactions explain the large spectral changes between types of solvent environments, but not the hypsochromic shifts within a solvent series of a single type. The molecular orbital character of the low and high energy transitions resembles those of OB, as illustrated in Figure 8. The HOMO and HOMO-2 orbitals show electron density on both ring moieties, likely due to the presence of a hydroxyl group on each ring. The low energy transition is predominantly HOMO to LUMO and is accompanied by a change in electron density near the hydroxyl and carbonyl groups, which supports an ESPT following photoexcitation to the S_1 state. The high energy transition is characterized as HOMO-2 to LUMO and is localized on the ring moieties, showing π to π^* character. Consideration of the potential energy surface and Franck−Condon transitions for the electronic states provides a more complete model for the solvatochromic trends than dipole moments alone.[44] The potential surfaces for the electronic states before and after the charge transfer are horizontally displaced relative to one another with respect to the equilibrium coordinates for the solute and solvent environment. More polar solvents have greater electrostatic interactions with the solute, resulting in a more pronounced change in the equilibrium positions upon going from the ground state to the excited charge transfer state. For DOB the horizontal displacement of the potential wells offsets the vertical stabilization, based upon the polarity of the electronic states. The net result is a higher energy Franck−Condon transition from the equilibrium ground state vertically to the first excited state or a blue shift with increasing solvent polarity.

4.1.3. Sulisobenzone. A hypsochromic shift is observed for SB with a significant blue shift (1500 cm^{-1}) upon going to electron pair donating solvents. The observed spectral shift does not correlate well with the solvatochromic models based upon parameters reported in Table 1. This may be indicative of different specific interactions outside of bulk dielectric effects or hydrogen bonding interactions. Within the protic solvents a small hypsochromic shift is observed likely due to changes in the dielectric constant of the solvent and displacement of the potential wells. There is minimal difference in the absorbance in nonhydroxylic solvents (hexanes) from those of the protic solvents. This result is similar to that observed in OB, as complexation with protic solvents at the carbonyl group will not result in significant structural changes for the SB. For this reason SB has similar absorbance properties in the presence (protic solvents) or absence (hexanes) of intermolecular hydrogen bonds at the carbonyl group. A large spectral shift is observed when explicit solvent−solute interactions may form in which the solvent can act as an electron pair donator. Such a change is not observed in OB, with the same intramolecular hydrogen bonding as SB, so it is reasoned that the interaction with the solvent is at the sulfonic acid group rather than the hydroxyl group.

Solutions of SB are acidic, pH of 4 at the concentrations studied, indicating deprotonation at the sulfonic acid group. A potential deviation in the electron pair donating solvents from other solvents is whether or not the solvent is able to solvate the acidic proton or if the proton is associated with the SB. Calculations indicate that the anion is anticipated to have a lower excitation ($S_0 \rightarrow S_1$) energy than the neutral species. Association of the proton at the carbonyl group of SB results in a decrease in the excitation energy relative to the fully deprotonated anion. In electron pair donating solvents, the solvent can readily solvate the proton and it is favorable for the proton to not be in the vicinity of the anion. Basicity scales for solvents indicate that THF is more basic than CH_3CN, as the oxygen is more electronegative than nitrogen.[45] This would shift the equilibrium toward the anionic form of SB and a more pronounced spectral shift for THF. In contrast in solvents which do not readily solvate the free proton, the acidic proton of SB may form a hydrogen bond to the carbonyl group on SB. The result for the anion with the associated proton, a net neutral species, is a lower excitation energy than that of the fully deprotonated species. Previous investigations have shown that the carbonyl group of benzophenones can form a hydrogen bond to an acidic proton.[46]

In addition to the solvation of the free proton, spectral shifts may originate from electronic properties of SB due to conjugation between the suliso group and the hydroxyl groups. An electron-withdrawing group at the para-position enhances the acidity of the hydroxyl group through resonance conjugation. This enhancement strengthens hydrogen bonding at the hydroxyl for SB, relative to OB. In electron pair donating solvents, such as CH_3CN and THF, this strengthens solvent−solute interactions. Calculations of the solute−solvent complexes do not indicate significant structural changes due to this interaction, but there is an increase in the length of the intramolecular hydrogen bond between the hydroxyl and carbonyl groups. The ZINDO excitation energy calculations indicate increased excitation energies, but not as large as the experimentally observed shifts, for the THF and CH_3CN complexes of SB. Smaller blue shifts are calculated for the same complexes of OB. To further analyze acidic versus electronic effects, other electron withdrawing groups, lacking acidic protons, may be analyzed.

4.2. Excited-State Reactivity. The viability of the intramolecular ESPT mechanism was evaluated for each of the compounds, as this is a primary proposed mechanism for the

efficient decay of the excited chromophore back to its ground state and relative photostability.[17] In OB and SB, where there is only one intramolecular hydrogen bond, an ESPT is thermodynamically favorable. In contrast in DOB, where there are two intramolecular hydrogen bonds to the central carbonyl, the ESPT is not favorable to either ring moiety. For all species, excitation energy calculations indicate the low energy electronic transition is HOMO to LUMO in character and results in a change in the electronic character at the hydroxyl and carbonyl groups. This is in agreement with previous assignments for *o*-hydroxy-substituted benzophenones, resembling OB without the methoxy substituent.[20,24] There is a shift in electron density to the central carbonyl with the $S_0 \rightarrow S_1$ excitation, promoting the transfer of the proton from the hydroxyl group to that of the carbonyl, supporting an ESPT. In DOB, for which there are two intramolecular hydrogen bonds to the central carbonyl, the extent of the transfer may be reduced from that of OB and SB which have only one intramolecular hydrogen bond.

The possibility of the intermolecular ESPT was not explicitly considered for the systems but would be a possibility for all species in protic solvents. The formation of intermolecular hydrogen bonded complexes is energetically favorable for OB and SB based upon calculations and experimentally supported by the spectral shifts of DOB. Previous studies indicate variations in the electronic transitions of *o*-hydroxyl benzophenones, similar to OB, in hydroxylic versus nonhydroxylic solvents indicative of intermolecular hydrogen bond formation.[24] Evaluation of the excited state lifetimes of the systems and solvent effects upon the lifetimes would complement the calculations of the thermodynamics of the intramolecular ESPT process.

5. Conclusions

The solvatochromic behavior of the series of benzophenone derivatives, all FDA approved for use as sunscreen active ingredients in personal care products, shows significant solvent-dependent absorbance properties. For OB, the most commonly used chemical in the series, solvent−solute interactions do not have a significant impact upon the observed spectral properties. Calculations support the formation of solvent−solute complexes, but minimal structural changes accompany complexation and excitation energies are not affected. Additionally, the ESPT that is proposed to result in the photostability of the product is found to be thermodynamically favorable and supported by the charge transfer character of the lowest energy ($S_0 \rightarrow S_1$) electronic transition. Similar results are found for SB, with the exception of its behavior in electron pair donating solvents. Weakly basic solvents, such as THF and CH_3CN, are able to solvate the acidic proton to a greater extent resulting in the dominant form of SB as the fully deprotonated anion. In other solvents the acidic proton remains associated with the SB. DOB shows the greatest solvent dependence in its photophysical behavior. Formation of explicit solvent−solute complexes with both protic and electron pair donating solvents results in an increased torsion angle between the ring moieties and an increased excitation energy for the complexed form relative to that of the free species. A complete ESPT is not thermodynamically favorable for DOB, but examinations of the molecular orbitals and spectral shifts do indicate charge transfer character in the lowest energy electronic transition.

The results of this investigation indicate the importance of the solvent−solute interactions upon the photophysical properties and enrich the fundamental understanding of the origin, at a molecular level, of the unique spectral properties of the benzophenone derivatives. This is particularly valuable for the formulation of personal care products utilizing the molecules' absorbance properties, as well as understanding their potential environment impact. Molecular level changes resulting from interactions of the solvent and solute must be considered to fully understand the photophysical properties of these commercially relevant compounds.

Acknowledgment. The authors thank the College of Wooster for support of this research through Start-Up funds and the Sophomore Research Program. This work was supported in part by a grant to The College of Wooster from the Howard Hughes Medical Institute through the Undergraduate Science Education Program. Additionally S.J.S. thanks Professor David Modarelli at the University of Akron for useful conversations regarding this research.

Supporting Information Available: Comparison of optimized structures of the DOB:MeOH complex with and without inclusion of the IEF-PCM solvation model, representative solvent complexes of the benzophenones, table of oscillatory strengths, and integrated absorbance areas for the benzophenones in a range of solvents. This information is available free of charge via the Internet at http://pubs.acs.org.

References and Notes

(1) Jeffrey, G. *An Introduction to Hydrogen Bonding*; Oxford University Press, Inc.: New York, 1997.
(2) Grunwald, E.; Eustace, D. Participation of hydroxylic solvent molecules. In *Proton-Transfer Reactions*; Caldin, E., E., Gold, V., Eds.; John Wiley & Sons: New York, 1975; pp 103−120.
(3) Zheng, J.; Fayer, M. D. *J. Am. Chem. Soc.* **2007**, *129*, 4328–4335.
(4) Kool, E. T. *Annu. Rev. Biophys. Biomol. Struct.* **2001**, *30*, 1–22.
(5) Dong, J.; Solntsev, K. M.; Tolbert, L. M. *J. Am. Chem. Soc.* **2006**, *128*, 12038–9.
(6) Kong, X. H.; Deng, K.; Lang, Y. L.; Zeng, Q. D.; Wang, C. *J. Phys. Chem. C* **2007**, *111*, 17382–17387.
(7) Taylor, C. A.; El-Boyoumi, M. A.; Kasha, M. *Proc. Natl. Acad. Sci. U.S.A.* **1969**, *63* (2), 253–260.
(8) Mente, S.; Maroncelli, M. *J. Phys. Chem. A* **1998**, *102*, 3860–3876.
(9) Sobolewski, A. L.; Domcke, W. *J. Phys. Chem. A* **2007**, *111* (46), 11725–11735.
(10) Robinson, B. H. Hydrogen-bonding and proton-transfer reactions in aprotic solvents. In *Proton-Transfer Reactions*; Caldin, E., Gold, V., Eds.; John Wiley & Sons: New York, 1975; pp 121−152.
(11) Morillo, M.; Cukier, R. I. *J. Chem. Phys.* **1990**, *92* (8), 4833–4838.
(12) Burghardt, I.; Hynes, J. T. *J. Phys. Chem. A* **2006**, *110*, 11411–11423.
(13) Schmidtke, S. J.; Underwood, D. F.; Blank, D. A. *J. Phys. Chem. A* **2005**, *109* (32), 7033–7045.
(14) Skin Deep Cosmetic Safety Database. http://www.cosmeticsdatabase.com/special/sunscreens/active.php.
(15) Reisch, M. S. *Chem. Eng. News* **2005**, *83* (15), 18–22.
(16) Shaath, N. A. The Chemistry of Sunscreens. *Cosmet. Sci. Technol. Ser.* **1990**, *10*, 211–33.
(17) Gasparro, F. P.; Mitchnick, M.; Nash, J. F. *Photochem. Photobiol.* **1998**, *68* (3), 243–56.
(18) Richardson, S. D. *Anal. Chem.* **2006**, *78*, 4021–46.
(19) Vanderford, B. J.; Pearson, R. A.; Rexing, D. J.; Snyder, S. A. *Anal. Chem.* **2003**, *75*, 6265–74.
(20) Hrdlovič, P.; Schubertová, N.; Palovčík, R. *Collect. Czech. Chem. Commun.* **1971**, *36* (5), 1942–7.
(21) Kysel, O. *Collect. Czech. Chem. Commun.* **1974**, *39* (11), 3256–67.
(22) Lamola, A. A.; Sharp, L. J. *J. Phys. Chem.* **1966**, *70* (8), 2634–8.
(23) Beyere, L.; Yarasi, S.; Loppnow, G. R. *J. Raman Spectrosc.* **2003**, *34*, 743–50.
(24) Dilling, W. L. *J. Org. Chem.* **1966**, *31* (4), 1045–1050.
(25) Agrapidis-Polympis, L. E.; Nash, R. A.; Shaath, N. A. *J. Soc. Cosmet. Chem.* **1987**, *38*, 209–21.
(26) Gaspar, L. R.; Campos, P. M.; Maia, B. G. *Int. J. Pharm.* **2007**, *343* (1−2), 181–9.
(27) Fung, S. Y.; Duhamel, J.; Chen, P. *J. Phys. Chem. A* **2006**, *110*, 11446–54.
(28) Kiprianov, A. *Russ. Chem. Rev.* **1960**, *29*, 618–26.
(29) Cramer, C.; Truhlar, D. *Chem. Rev.* **1999**, *99* (8), 2161–200.

(30) Schmidtke, S. J.; MacManus-Spencer, L. A.; Klappa, J. J.; Mobley, T. A.; McNeill, K.; Blank, D. A. *Phys. Chem. Chem. Phys.* **2004**, *6* (15), 3938–47.

(31) MacManus-Spencer, L. A.; Schmidtke, S. J.; Blank, D. A.; McNeill, K. *Phys. Chem. Chem. Phys.* **2004**, *6* (15), 3948–57.

(32) Cramer, C. *Essentials of Computational Chemistry*, 2nd ed.; John Wiley and Sons, Ltd.: Hoboken, NJ, 2004.

(33) Frisch, M. J.; Trucks, G. W.; Schlegel, H. B.; Scuseria, G. E.; Robb, M. A.; Cheeseman, J. R.; Montgomery, J. A., Jr.; Vreven, T.; Kudin, K. N.; Burant, J. C.; Millam, J. M.; Iyengar, S. S.; Tomasi, J.; Barone, V.; Mennucci, B.; Cossi, M.; Scalmani, G.; Rega, N.; Petersson, G. A.; Nakatsuji, H.; Hada, M.; Ehara, M.; Toyota, K.; Fukuda, R.; Hasegawa, J.; Ishida, M.; Nakajima, T.; Honda, Y.; Kitao, O.; Nakai, H.; Klene, M.; Li, X.; Knox, J. E.; Hratchian, H. P.; Cross, J. B.; Bakken, V.; Adamo, C.; Jaramillo, J.; Gomperts, R.; Stratmann, R. E.; Yazyev, O.; Austin, A. J.; Cammi, R.; Pomelli, C.; Ochterski, J. W.; Ayala, P. Y.; Morokuma, K.; Voth, G. A.; Salvador, P.; Dannenberg, J. J.; Zakrzewski, V. G.; Dapprich, S.; Daniels, A. D.; Strain, M. C.; Farkas, O.; Malick, D. K.; Rabuck, A. D.; Raghavachari, K.; Foresman, J. B.; Ortiz, J. V.; Cui, Q.; Baboul, A. G.; Clifford, S.; Cioslowski, J.; Stefanov, B. B.; Liu, G.; Liashenko, A.; Piskorz, P.; Komaromi, I.; Martin, R. L.; Fox, D. J.; Keith, T.; Al-Laham, M. A.; Peng, C. Y.; Nanayakkara, A.; Challacombe, M.; Gill, P. M. W.; Johnson, B.; Chen, W.; Wong, M. W.; Gonzalez, C.; Pople, J. A. *Gaussian 03, Revision C.02*; Gaussian, Inc.: Wallingford, CT, 2004.

(34) Becke, A. D. *J. Chem. Phys.* **1993**, *98*, 5648–5652.

(35) Perdew, J. P.; Burke, K.; Wang, Y. *Phys. Rev. B* **1996**, *54*, 16533.

(36) Easton, R.; Giesen, D.; Welch, A.; Cramer, C.; Truhlar, D. *Theor. Chim. Acta* **1996**, *93* (5), 291–301.

(37) Stratmann, R.; Scuseria, G.; Fritsch, M. *J. Chem. Phys.* **1998**, *109* (19), 8218–8224.

(38) Bauernschmitt, R.; Alhlrichs, R. *Chem. Phys. Lett.* **1996**, *256* (4,5), 454–464.

(39) Dennington, Roy, II; Keith, Todd; Millam, John; Eppinnett, Ken; Hovell, W. Lee; Gilliland, Ray *GaussView, Version 3.09*; Semichem, Inc.: Shawnee Mission, KS, 2003.

(40) Thompson, M. A. *ArgusLab 4. 0 1* Planaria Software LLC: Seattle, WA, http://www.arguslab.com.

(41) Winget, P.; Dolney, D.; Giesen, D.; Cramer, C.; Truhlar, D. G. Minnesota solvent descriptor database; Department of Chemistry and Supercomputer Institute, University of Minnesota: Minneapolis, MN, 1999.

(42) Reichardt, C. *Chem. Rev.* **1994**, *94* (8), 2319–2358.

(43) Kamlet, M. J.; Abboud, J. L. M.; Abraham, M. H.; Taft, R. W. *J. Org. Chem.* **1983**, *48* (17), 2877–2887.

(44) Kiprianov, A. I. *Russ. Chem. Rev.* **1960**, *29*, 618–626.

(45) Catalán, J.; Palomar, C. D.; de Paz, J. L. G. *J. Phys. Chem. A* **1997**, *101*, 5183–5189.

(46) Stasko, D.; Hoffmann, S. P.; Kim, K. C.; Fackler, N. L. P.; Larsen, A. S.; Drovetskaya, T.; Tham, F. S.; Reed, C. A.; Rickard, C. E. F.; Boyd, P. D. W.; Stoyanov, E. S. *J. Am. Chem. Soc.* **2002**, *124*, 13869–13876.

JP810256X